- Technical Paper -

Numerical Collapse Analysis of Tsuyagawa Bridge Damaged by Tohoku Tsunami

Hamed SALEM[1], Suzan MOHSSEN[2], Yuto NISHIKIORI [3] and Akira HOSODA[4]

ABSTRACT

The collapse of Tsyuagawa bridge damaged by Tohoku Tsunami is numerically investigated using the Applied element Method, due to its advantages of simulating structural progressive collapse. The analysis was proven to simulate the bridge collapse. It showed that the bridge collapsed at a water speed of 6.6 m/sec initiated by flexural failure of its piers. Study of bridge strengthening showed that the collapse water speed could be increased by 22% and 29% compared to Tohoku tsunami if the piers are strengthened by a 100-mm RC jacket and 20-mm thick steel jacket, respectively.

Keywords: Tohoku tsunami; progressive collapse; applied element method

1. INTRODUCTION

On March 11th, 2011, the Tohoku tsunami, with 10m-high waves swept over the east coast of Japan. The Japanese National Police Agency confirmed 15,884 deaths, 6,150 injured, and 2,640 people missing, as well as 126,631 buildings totally collapsed, with a further 272,653 buildings 'half collapsed', and 743,492 buildings partially damaged. The violent shaking resulted in a nuclear emergency, in which the Fukushima Daiichi nuclear power plant began leaking radioactive steam. The estimated cost of the damage reached US$235 billion. The great Tohoku tsunami also caused widespread and severe structural damage to various infrastructures in north-eastern Japan, especially in the coastal area of Iwate, Miyagi, Fukushima and Ibaraki Prefectures. More than 250 bridges were washed away. As an example, Tsuyagawa Bridge in the Kesennuma line of JR-EAST suffered extensive damage by tsunami as shown in Fig.1, where the bridge decks were washed away and the RC piers were severely damaged by the tsunami forces (Kawashima et al., 2011).

The objective of the current study is to numerically investigate the collapse mechanism of Tsuyagawa bridge and propose structural design enhancements to avoid such collapse in future under similar tsunami. The choice of the numerical method to do such investigation was very important because of the significant need to simulate the collapse of different parts of the bridge to the end. Although the FEM is a robust and well established structural analysis method, it is not the optimum solution for the current study scope. Many drawbacks are associated with the FEM progressive collapse analysis; the element damage separation, falling and collision with other elements are very difficult (Hartmann *et al.*, 2008). Therefore, in the current study, the numerical analysis was carried out using the Applied Element Method. The Applied Element Method is based on discrete crack approach and is capable of following the structure's behavior to its total collapse (Tagel-Din and Meguro, 2000, Meguro and Tagel-Din, 2001, Tagel-Din, 2002, Meguro and Tagel-Din, 2003, Sasani and Asgitoglu, 2008, Salem et al., 2011, Park et al., 2009, Helmy et al., 2009, Helmy et al., 2012, Helmy et al., 2013, Sasani, 2008, Wibowo, 2009, Salem 2011, Salem and Helmy, 2014, Salem et al., 2014).

2. COLLAPSE OF TSUYAGAWA BRIDGE

Tsuyagawa bridge consisted of 7 spans with 6 prestressed simply supported girders (35m+40m×5) and 1 RC girder (22m). Seven conical piers and one abutment supported the bridge superstructure. The superstructures for 6 spans were completely washed away from their supports in the transverse direction due to tsunami while four of the supporting piers (P2, P3, P4 and P6) were extensively damaged as shown in Fig. 1. The bearings remained attached to the pier after the wash away of the superstructure.

3. THE APPLIED ELEMENT METHOD (AEM)

The AEM is an innovative modeling method adopting the concept of discrete cracking. In AEM, structures are modeled with elements assembly as shown in Fig. 2. The elements are connected together along their surfaces through a set of normal and shear springs. Those springs are responsible for transfer of normal and shear stresses among adjacent elements. Each spring represents stresses and deformations of a certain volume of the material as shown in Fig. 2. Each two adjacent elements can be completely separated once the springs connecting them are ruptured.

Fully nonlinear path-dependent constitutive models are adopted in the AEM as shown in Fig. 2. For

[1] Professor of concrete structures, Cairo University, Egypt
[2] Structural engineer, Applied Science International, Cairo, Egypt
[3] Oriental Consultants Co., Ltd. , Japan
[4] Associate professor, Faculty of Urban Innovation, Yokohama National University, Japan

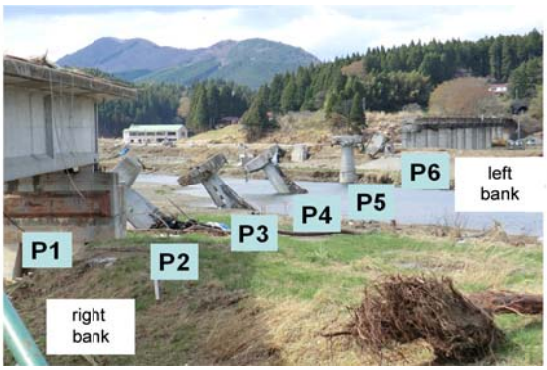

Fig.1 Collapsed Tsuyagawa Bridge, due to Tohoku Tsunami

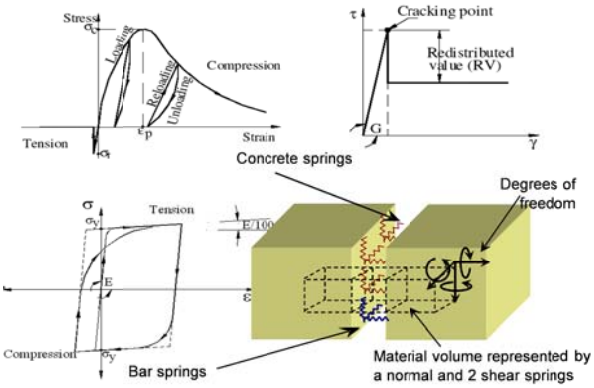

Fig.2 Modeling of a structure with the AEM

concrete in compression, elasto-plastic and fracture model is adopted (Maekawa and Okamura, 1983). When concrete is subjected to tension, linear stress-strain relationship is adopted until cracking, where the stresses drop to zero. Since the method adopts discrete crack approach, the reinforcing bars are modeled as bare bars for the envelope (Okamura and Maekawa, 1991) while the model of Ristic *et al.* (1986) is used for the interior loops.

As for the bearing modeling, an interface material model is used. The interface material model is a pre-cracked model where the material is initially cracked and can not carry tensile stresses. As for compression, the stress-strain relation is linear up to compression failure stress. The relationship between shear stress and shear strain is assumed linear till the shear stress exceeds $\mu\ \sigma_n$ (coefficient of friction times normal stress) where the shear stress remains with this value ($\mu\ \sigma_n$) as long as normal stresses are not changed. Again, increasing the compressive stresses will make shear stresses to increase again till shear stresses reach ($\mu\ \sigma_n$). The shear stiffness is set as minimum if the crack is open or during sliding.

The AEM is a stiffness-based method, in which an overall stiffness matrix is formulated and the equilibrium equations including each of stiffness, mass and damping matrices are nonlinearly solved for the structural deformations (displacements and rotations). The solution for equilibrium equations is an implicit one that adopts a dynamic step-by-step integration (Newmark-beta time integration procedure) (Bathe, 1982 and Chopra, 1994).

In the AEM, two adjacent elements can separate from each other if the matrix springs connecting them are ruptured. Elements may automatically separate, re-contact or contact other elements. In this study, the Extreme Loading for Structures (ELS) software (www.appliedscienceint.com), which is based on the AEM, is used.

The AEM was proven to be capable of following the deformations of a structure subjected to extreme loads to its total collapse. Therefore, and since the goal of the current study is to investigate the behavior of reinforced concrete structures under severe loads resulting from tsunami action, it was decided that the AEM is the most appropriate numerical tool for such investigation. Although the Finite Element Method (FEM) is a robust and well established structural analysis method, it is not the optimum solution for the scope of progressive collapse analysis. Many drawbacks are associated with the FEM progressive collapse analysis. The elements damage, separation, falling and collision with other elements are very difficult. Hartmann *et al.* (2008) showed that the computations associated with the simulation of collapses of real world structures based on conventional FEM are very costly, and therefore followed another approach based on multibody models.

4. BRIDGE ANALYTICAL MODEL

4.1. Structural Model

The bridge was modeled using Extreme Loading for Structures software (ELS, www.appliedscienceint.com). The model included concrete and reinforcement details of the bridge superstructure, i.e, slabs, girders and piers. The foundations were not modelled and the piers were assumed totally fixed to their foundations. This assumption matches the reality where the collapse of the bridge did not experience any tilting of the pile caps assuring high rigidity, moreover, no soil scouring was recognized or reported.

The structural drawings available for bridge were very old and many reinforcement details could not be clearly obtained, therefore, a site investigation was carried out to completely detect reinforcing bars arrangement. As a sample, Fig. 3 shows investigated bars arrangement of piers P2~P5. Bars cut-off at the top of piers were observed and considered in the numerical model.

Each deck was simply supported on two groups of bearing, one was fixed while the other was movable as shown in Fig. 4(a). The bearings were modeled as shown in Fig. 4, where each bearing is composed of a bottom bed plate and a top sole plate. The top sole plate of the fixed bearings has two edges that block with the bed plate and thus prevents longitudinal movement of the deck, while that of the movable bearings has not such a kind of edges. In the movable bearings, a neoprene plate was also located between the sole and bed plates to reduce friction and allow for longitudinal movements. In the AEM model, the value of friction coefficient between the sole and bed plates was put as 0.6 and zero for fixed and movable bearings,

respectively. In both bearings, side block was fixed to the bed plate through bolts to prevent the lateral movements of the deck. For simplicity, the bolts were not explicitly modeled, and alternatively the interface between the side blocks and the bed plate was put that its strength is equal to that of the bolts. Fig. 5 shows the whole modeled bridge. A mesh sensitivity analysis was carried out for different structural components to get the minimum number of elements sufficient for a good accuracy.

4.2. Material properties

Table 1 shows the material properties adopted in the AEM analysis. The bearing interface is given a relatively high compressive strength so that it does not fail in compression but behave linearly. The interface between the neoprene and sole plate or bed plate is given a bearing material with the neoprene modulus of elasticity and compressive strength.

The friction coefficient between the sole and bed plates was put as 0.6 and zero for fixed and movable bearings, respectively. The interface between the side block plate and the bed plate is given the modulus of elasticity and strength of the connecting bolts divided by the contact area of the side block and the bed plate.

4.3. Main Assumptions

1. Water velocity and inundation depths are adopted from calculations of Li et al. (2013). Fig.6 shows water velocity, and water height acted on the bridge. The most sever combination of inundation depth and water speed was at 44 minutes and 20 seconds, when water covered the top of the decks while its speed was 6.6 m/sec (99% of maximum water speed).

2. Bricker et al. (2012) carried out two-dimensional computational fluid dynamic analysis to the deck of Utatsu Ohashi bridge and found out that, air is trapped between girders during motion of water. This trapped air causes additional buoyant forces that are essential to be considered in the analysis. The trapped air between girders was considered following the simplified model adopted by Salem et al. (2014), where the trapped air height is linearly proportional to the speed of water and reaches 100% of the clear depth of the girders when speed reaches 3.13 m/sec.

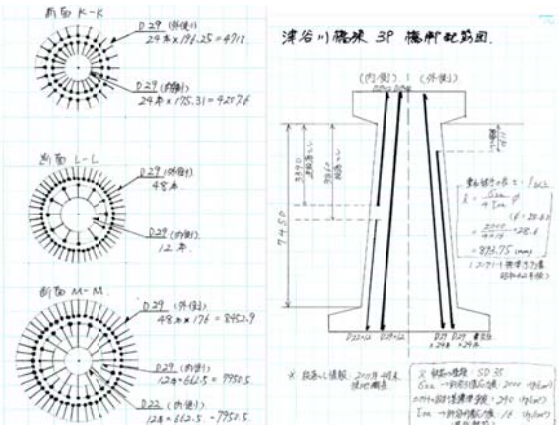

Fig.3 Investigated bars arrangement of piers P2~P5

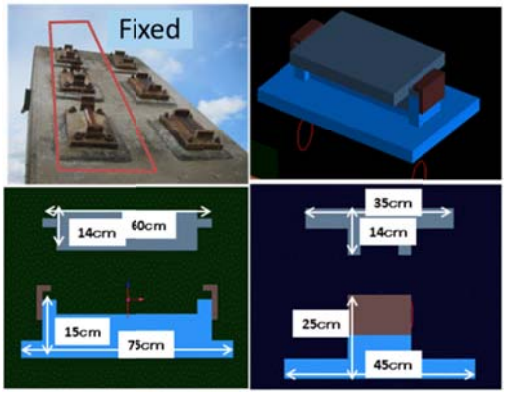

(a) Geometry of bearings

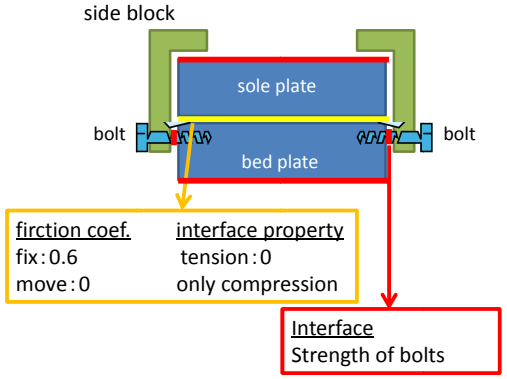

(b) Material properties for the interfaces of bearing

Fig.4 AEM model of bridge bearings

Table.1 Material properties

Material	Young's mod. (MPa)	Comp str. (MPa)	Tens. str. (MPa)	Yield/ Ult.Str. (MPa)
Concrete	26717	30	3	----
Steel	203890	----	----	360/504
Bearing	203890	540	0	----
Mov. bearing	26716	30	0	----
Side interface	14741	540	22	----

4.4. Tsunami Loads Acting on the Bridge

Tsunami loads considered to be acting on the bridge are the drag forces (hydrodynamic forces) and the buoyant forces (uplift forces). Surge (impulsive) forces are of low effect because they are caused by the leading edge of the water surge and at that stage the water height is low and have little effect on the superstructure.

4.5. Hydrodynamic Force

Hydrodynamic (drag) forces act when water flows around the bridge. They include frontal impact on the upstream face, drag along the sides, and suction on the downstream side. These forces are induced by the flow of water moving at moderate to high velocity, and are a function of fluid density, flow velocity and structure geometry. Hydrodynamic forces can be computed as follows (JSCE, 2007 and FEMA ,2008):

$$F_d = \frac{1}{2}\rho_s C_d A V^2 \qquad (1)$$

where
F_d = Horizontal drag (hydrodynamic) force
C_d = Drag coefficient $\cong$ 2.0 (FEMA ,2008)
ρ_s = density of sea water including sediments (= 1.2 density of sea water, FEMA ,2008) and V= velocity of water
A= Area of structural member normal to flow

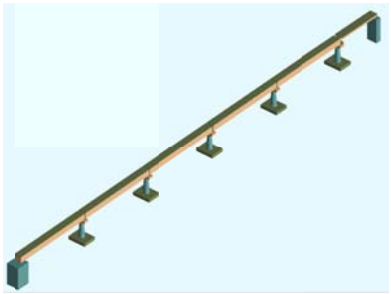

Fig.5 AEM model of the whole bridge

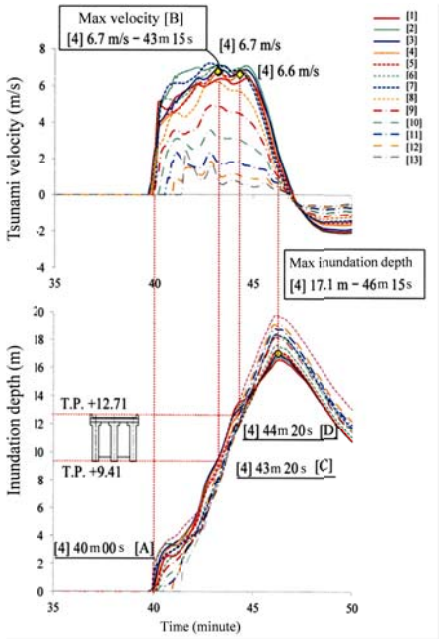

Fig. 6 Water speed and inundation depth (Li al., 2013)

It is herein important to understand that this equation assumes that the object around which water flows is a stationary object and the water flows around with a velocity "V". The bridge deck could be stationary in the beginning of the tsunami attack but when it starts to slide and move, it will be a moving object. Therefore, the velocity "V" would be the relative velocity between the water and the bridge deck. Since ELS is pure structural analysis software and has no coupled fluid-structural dynamics solver, Salem et al. (2014) adopted a simplified iterative method, which is used here, to consider the correct pressure acting on the bridge. First of all, the pressure is calculated based on the water velocity given by Li et al (2013). From the AEM analysis, the velocity of the bridge deck is obtained, and hence the relative velocity between the water flow and the bridge deck is recalculated and the hydrodynamic pressure is also recalculated. With the new calculated hydrodynamic pressure, the AEM analysis is carried out again and the velocity of the moving deck is recalculated. These steps are repeated till reaching a non-changeable pressure values. Fig.7 shows a sample for pressure calculation.

4.6. Buoyant Force

The buoyant force's magnitude equals to the weight of the volume of water displaced by the submerged body. Buoyant forces are calculated as follows:

$$F_b = \rho_s g V_D \quad (2)$$

where
F_b = Buoyant Force
V_D= volume of water displaced by the submerged object (bridge deck)
ρ_s = density of sea water including sediments (= 1.2 density of sea water) and g= gravitational acceleration

The buoyant force was considered in the model by reducing the unit weight of the bridge concrete by a magnitude equals the unit weight of the sea water.

Bricker et al. (2012) carried out two-dimensional computational fluid dynamic analysis to the deck of Utatsu Ohashi bridge and found out that, air is trapped between girders during motion of water. This trapped air between girders (Bricker et al., 2012) causes additional buoyant forces that are taken into consideration applying additional buoyant forces equal to the weight of the volume of water displaced by the trapped air and is calculated as follows:

$$F_{bT} = \rho_s g V_{AT} \quad (3)$$

where
F_{bT} = Buoyant Force due to trapped air
V_{AT}= volume of water displaced by the trapped air
ρ_s = density of sea water including sediments (= 1.2 density of sea water, FEMA ,2008)
g= gravitational acceleration

These forces are considered by being directly applied to the deck slab in the upward vertical direction, and when the bridge decks are overturned, analysis is repeated considering those buoyant forces to reduce to zero when the deck rotation reaches 90 degrees. It is believed that at this stage the trapped air would be released.

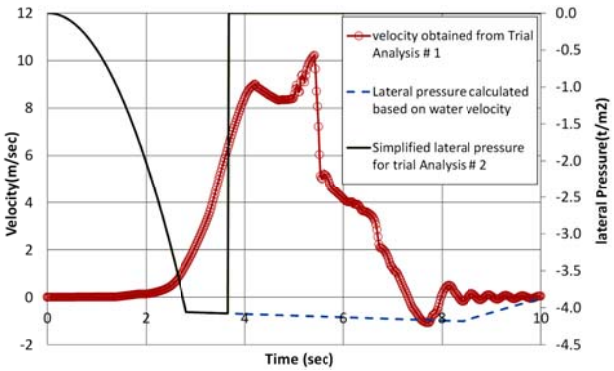

Fig.7 A sample for pressure simplified calculations

5. RESULT OF AEM ANALYSIS

5.1. Behavior of Tsuyagawa bridge under the tsunami action

Analytical results of Tsuyagawa bridge under the tsunami action have shown that the bridge started being tilted at a water speed of 6.6 m/sec. Due to this tilt, piers initially collapsed leading to washing away of the decks as shown in Fig. 8. Only pier P6 collapsed at reinforcement cut-off part, while pier P5 collapsed at the middle of its height and other piers collapsed at the bottom sections. Failure mode was in general close to reality observed after tsunami hit, however, in analysis Piers P2, P3 and P4 were completely separated from foundations indicating less ductility than in reality.

Collapse of piers was initiated by the rupture of reinforcing bars. Fig.9 shows normal stresses in the most stressed bars at the failure sections of piers P4, P5 and P6, respectively, where it is found that the normal stresses exceeded the ultimate strength of reinforcing bars, leading to pier collapse.

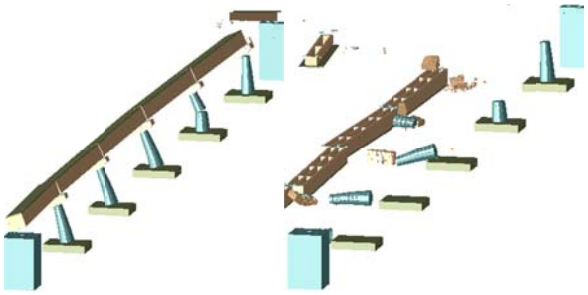

(a) t= 3.78 sec (b) t= 9.5 sec

Fig.8 AEM results for bridge collapse

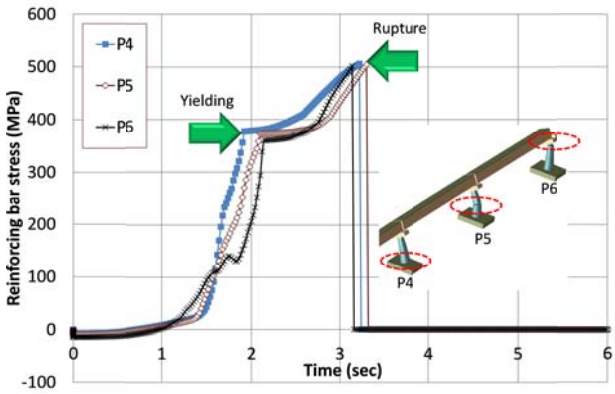

Fig. 9 Normal stresses in the most stressed bars at the failure sections of piers P4, P5 and P6

5.2. Investigation of different strengthening techniques of Tsuyagawa bridge

In this section, an investigation of different pier strengthening techniques on the behavior of Tsuyagawa bridge under tsunami action is carried out. This could be beneficial to existing similar bridges that need rehabilitation to withstand against possible future tsunamis or in general for the design of new bridges in coastal areas in Japan. Four cases were studied. In the first case, the original pier reinforcement configuration is modified and a continuous reinforcement is used as a replacement of the cut-off of re-bars. In the second case, a huge reinforced concrete jacket is used with a thickness that doubles the original pier dimensions with an average reinforcement ratio of 3.7%. In the third case, 100-mm thick reinforced concrete jacket with a reinforcement ratio of 8.3% is studied, while in the fourth case a 20-mm thick steel jacket, fully anchored to the footing, is used.

In this parametric study, the speed of water is not limited to the recorded speed that hit Tsuyagawa bridge during the 2011 Tohuku Tsunami. The objective of the study is to get the maximum water speed that can be resisted by the strengthened bridge. Fig.10 shows the collapse mode obtained by the AEM model. As seen in Fig. 10, cases 1 and 3 experienced flexural failure at the bottom sections of the pier eliminating the failure at the top cut-off part. On the other hand, case 2 with the huge reinforced concrete jacketing experienced a bearing failure eventually led to deck sliding while piers remained in place. Fig.11 shows the collapse sequence of the bearing plates. In case 4, the existence of such a steel jacket prevented the collapse of the pier, however, the collapse took place the bottom part of the girder supporting the bridge decks as shown in Fig. 10(d). The water speeds that caused failure of the bridge for different strengthened cases are shown in Fig. 12.

6. CONCLUSIONS

The AEM analysis of Tsuyagawa bridge was proven to efficiently simulate its collapse due to the 2011 Tohoku Tsunami, in spite that, the analytical results showed less ductility compared to reality. Analytical results showed that the bridge collapsed at a water speed of 6.6 m/sec initiated by the flexural failure of bridge piers.

Numerical investigation of strengthening technique showed that the proposed strengthening techniques could enhance the tsunami-resistance of similar bridges. The collapse tsunami water speed could be increased by 22% and 29% compared to Tohoku tsunami if the piers are strengthened by a 100-mm reinforced concrete jacket and 20-mm thick steel jacket, respectively.

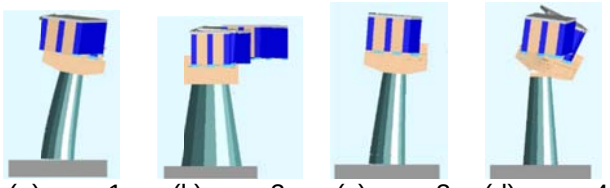

(a) case 1 (b) case 2 (c) case 3 (d) case 4

Fig.10 Numerical results for different strengthening techniques

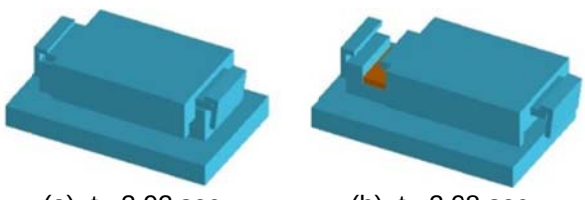

(a) t= 2.92 sec (b) t= 2.98 sec

Fig.11 Collapse of the bearing plates in case 2

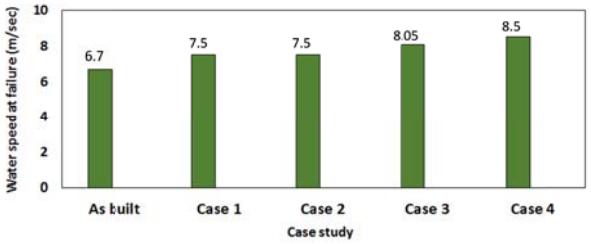

Fig.12 Water speed causing failure of the bridge for different strengthened cases

REFERENCES

1) Applied Science International, LLC (ASI) www.appliedscienceint.com
2) Bathe, K., *Solution of Equilibrium Equations in Dynamic Analysis*. Prentice Hall, Englewoods Cliffs, N.J., 1995
3) Bricker, J., Kawashima, K. and Nakayama, A., "CFD analysis of bridge deck failure due to tsunami", *Proceedings of the International Symposium on Engineering Lessons Learned from the 2011 Great East Japan Earthquake*, March 1-4, 2012, Tokyo, Japan
4) Chopra, A., *Dynamics of Structures: Theory and Applications to Earthquake Engineering*. Prentice Hall, Englewoods Cliffs, N.J., 1995
5) FEMA, *Guidelines for Design of Structures for Vertical Evacuation from Tsunamis*, FEMA P646 Report, prepared by the Applied Technology Council for the Federal Emergency Management Agency, 2008, Redwood City, California
6) Hartmann, D., Breidt, M., Nguyen, V., Stangenberg, F., Hohler, S., Schweizerhof, K., Mattern, S., Blankenhorn, G., Moller, B., and Liebscher, M. (2008), Structural Collapse Simulation under Consideration of Uncertainty – Fundamental Concept and Results, *Computers and Structures*, 86, 2064–2078.
7) Helmy H., Salem H., Tageldin H., Numerical simulation of Charlotte Coliseum demolition using the Applied Element Method. *USNCCM-10 conference-Ohio-USA*, 2009.
8) Helmy, H., Salem, H. and Mourad, S., Progressive collapse assessment of framed reinforced concrete structures according to UFC guidelines for alternative path method, *Engineering Structures*, 2012, 42, 127–141.
9) Helmy, H., Salem, H. and Mourad, S., Computer-aided assessment of progressive collapse of reinforced concrete structures according to GSA Code, *Journal of performance of constructed facilities, ASCE*, October 2013 (In Press).
10) JSCE Standard Specifications for Concrete Structures "Design", No. 15, 2007
11) Kawashima, K., Kosa, K., Takabashi, Y., Akiyama, M., Nishioka, T., Watanabe, G., Koga, H. and Matsuzaki, H., Damage of Bridges during 2011 Great East Japan Earthquake, Retrieved July, 2012, http://www.nehrp.gov/pdf/UJNR-4217.pdf
12) Li, F., Kosa, K., Nakano, A., and Sasaki, T., Detailed Analysis of Damages in Utatsu Area by Tsunami, *The Proceedings of JCI*, Vol.35, No.2, 2013, 799-804
13) Maekawa, K. and Okamura, H., The Deformational Behavior and Constitutive Equation of Concrete using the Elasto-Plastic and Fracture Model, *Journal of the Faculty of Engineering, The University of Tokyo (B)*,1983, 37(2): 253-328.
14) Meguro, K., and Tagel-Din, H., Applied Element Simulation of RC Structures under Cyclic Loading, *ASCE*, 2001, 127(11), 1295-1305.
15) Meguro, K., and Tagel-Din, H., AEM used for Large Displacement Structure Analysis, *Journal of Natural Disaster Science*, 2003, 24(1), 25-34.
16) Meguro K, Tagel-Din H., Applied element simulation of RC structures under cyclic loading, *ASCE*, 2001, 127(11), 1295-1305.
17) Meguro K, Tagel-Din H., Applied element method for structural analysis: theory and application for linear materials, *Structural Eng./Earthquake Eng., International Journal of the Japan Society of Civil Engineers (JSCE);* 2000; 17(1); 21s-35s.
18) Okamura, H. and Maekawa, K., *Nonlinear Analysis and Constitutive Models of Reinforced Concrete*. Gihodo, Tokyo, 1991.
19) Park H, Suk C, Kim S., Collapse modeling of model RC structures using the Applied Element Method, *Journal of Korean Society for Roc Mechanics, Tunnel& Underground Space*, 2009, 19 (1), 43-51.
20) Ristic, D., Yamada, Y., and Iemura, H., Stress-Strain Based Modeling of Hysteretic Structures under Earthquake Induced Bending and Varying Axial Loads, *Research report No. 86-ST-01, 1986, School of Civil Engineering, Kyoto University,* Kyoto, Japan.
21) Salem H., Computer-aided design of framed reinforced concrete structures subjected to flood scouring, *Journal of American Science*, 2011, 7(10), 191–200.
22) Salem H, El-Fouly A, Tagel-Din, H., Toward an economic design of reinforced concrete structures against progressive collapse, *Engineering Structures*, 2011, 33, 3341-3350.
23) Salem, H. and Helmy, H. "Numerical investigation of collapse of the Minnesota I-35W bridge", Engineering Structures, 2014, 59, 635–645
24) Salem, H, Mohssen, S, Kosa, K, and Hosoda, A, "Collapse Analysis of Utatsu Ohashi Bridge Damaged by Tohuku Tsunami using Applied Element Method", Journal of Advanced Concrete Technology, 2014, Vol. 12(10), 388-402.
25) Sasani M, Sagiroglu S., Progressive collapse resistance of hotel San Diego. Journal of Structural Engineering, 2008, 134(3), 478-488.
26) Sasani M., Response of a reinforced concrete infilled-frame structure to removal of two adjacent columns, *Engineering Structures*, 2008, 30, 2478–2491.
27) Tagel-Din, H., and Meguro, K., Applied Element Method for dynamic large deformation analysis of structures, *Structural Engineering and Earthquake Engineering. Journal of the Japan Society of Civil Engineers (JSCE)*, 2000, 17(2): 215-224.
28) Tagel-Din, H., Collision of structures during earthquakes", *Proceedings of the 12th European Conference on Earthquake Engineering*, 2002, London, UK.
29) Tagel-Din H, Meguro K., Applied Element Method for simulation of nonlinear materials: theory and application for RC structures, *Structural Eng./Earthquake Eng., International Journal of the Japan Society of Civil Engineers(JSCE)*, 2000, 17(2), 123s-148s.
30) Tagel-Din H, Meguro K., Applied Element Method for dynamic large deformations analysis of structures, *Structural Eng./Earthquake Eng., International Journal of the Japan Society of Civil Engineers (JSCE)*, 2000, 17(2), 215s-224s.
31) Wibowo H, Reshotkina S, Lau D., Modelling progressive collapse of RC bridges during earthquakes, *CSCE Annual General Conference*, 2009, GC-176-1-11.